Global Change Biology (2006) **12,** 1253–1266, doi: 10.1111/j.1365-2486.2006.01170.x

Carbon isotope composition of fossil charcoal reveals aridity changes in the NW Mediterranean Basin

J. P. FERRIO*, N. ALONSO†, J. B. LÓPEZ†, J. L. ARAUS‡ and J. VOLTAS*

Departament de Producció Vegetal i Ciència Forestal, E.T.S.E.A-Universitat de Lleida, Av. Rovira Roure, 191, Lleida E-25198, Spain, †Group d'Investigació Prehistòrica, Departament d'Història, Universitat de Lleida, Pça. Víctor Siurana, 1, Lleida E-25003, Spain, ‡Unitat de Fisiologia Vegetal, Departament de Biologia Vegetal, Facultat de Biologia, Universitat de Barcelona, Av. Diagonal, 645, Barcelona E-08028, Spain

Abstract

Although several proxies for the inference of precipitation have been proposed, evidence of changes in aridity during the Holocene is scarce, and most is only qualitative. Moreover, precipitation regimes show relatively poor spatial correlations and can exhibit contrasting responses to global climate trends in different areas. Thus, there is a need to concentrate efforts at the local scale in order to increase the spatial resolution of palaeoclimate records, especially regarding water availability in semiarid zones. We propose the analysis of carbon isotope composition ($\delta^{13}C$) in fossil charcoal (routinely recovered from archaeological sites) to quantify changes in water availability in the past. We applied this approach to reconstruct variations in aridity during the last four millennia in the Ebro Depression (NE Iberian Peninsula). First, we studied the effect of carbonization over a range of temperatures (300–500 °C) on the $\delta^{13}C$ of Aleppo pine (*Pinus halepensis* Mill.) wood cores, collected from nine locations in NE Iberian Peninsula with distinct water availability. Despite significant changes in $\delta^{13}C$ caused by carbonization, the original climatic signal of wood $\delta^{13}C$ was well preserved. Moreover, $\delta^{13}C$ shifts induced by this process were successfully corrected by accounting for variation in charcoal carbon concentration (%C). After removing the effect of carbonization, we estimated annual precipitation (*P*) and the ratio between annual precipitation and evapotranspiration (*P*/*E*) from the $\delta^{13}C$ of fossil charcoal. In general, estimated water availability in the past was higher than present values, indicating that latter-day (semiarid) conditions are mostly due to recent climate changes. The good agreement between our findings and other evidence indicates that the analysis of $\delta^{13}C$ in charcoal may be useful to expand current palaeoclimate records as it provides a complementary (and quantitative) source of information to assess climate dynamics.

Keywords: archaeology, fossil wood, Iberian peninsula, late Holocene, palaeoclimate, *Pinus halepensis*, precipitation, proxy, stable isotopes, water availability

Received 14 December 2004; revised version received 5 October 2005; accepted 9 February 2006

Introduction

Global trends in temperature during the Holocene are well documented thanks to a variety of long-term, high-resolution proxy records (IPCC, 2001). In arid and semiarid areas, however, precipitation is the most relevant environmental variable determining the impact of climate fluctuations on ecosystems, agriculture, and human settlements. Although several proxies for precipitation have been proposed, most are only qualitative, and evidence of past changes in aridity during the Holocene is still scarce (IPCC, 2001). Moreover, and unlike temperature, precipitation regimes show relatively poor spatial correlations and can exhibit contrasting associations with global climate trends in different areas (e.g. Rodó *et al*., 1997). This is particularly evident for the Iberian Peninsula (NW Mediterranean Basin), where climate is defined by complex interactions between Atlantic, Mediterranean, Continental, and subtropical influences. Indeed, a great spatial heterogeneity in the response to global climate trends has been

Correspondence: Jordi Voltas, tel. + 34 973 702622, fax + 34 973 23 82 64, e-mail: jvoltas@pvcf.udl.es

reported for the Iberian Peninsula, both in present climatic data (Rodó *et al*., 1997) and in the palaeoenvironmental record (Davis, 1994; Jalut *et al*., 2000; Magny *et al*., 2003; Riera *et al*., 2004). Therefore, supplementary efforts should focus at the local scale in order to increase the spatial resolution of palaeoclimate records, especially regarding water availability in semiarid zones.

Carbon isotope composition ($\delta^{13}C$) in wood has been related to several climatic variables that affect plant water availability, and its analysis on tree rings offers the possibility of high-resolution climate records (see references in IPCC, 2001; Ferrio *et al*., 2003b; McCarroll & Loader, 2004). However, vast areas of the world have been largely deforested for a long period, thus precluding extensive tree-ring records. In this context, the analysis of the $\delta^{13}C$ from carbonized wood (charcoal) may provide useful information on past climates for these areas. Charcoal can be derived from either wildfires or human activities, and is relatively common within archaeological horizons, where it is systematically recovered and identified (e.g. February & Van der Merwe, 1992; Vernet *et al*., 1996; Willcox, 1999; Figueiral & Terral, 2002). Although numerous studies on the $\delta^{13}C$ of fossil plants and coals have been carried out, especially for deep geological times (see references in Gröcke, 1998), those focused on wood charcoal are still scarce (Jones, 1991; Jones & Chaloner, 1991; February & Van der Merwe, 1992; Vernet *et al*., 1996). Likewise, the abundance of experimental works devoted to the effect of postburial degradation on wood $\delta^{13}C$ (e.g. Schleser *et al*., 1999; Van Bergen & Poole, 2002; further references in Gröcke, 1998; Gröcke, 2002) contrasts with the scarcity of isotope studies on experimental modern charcoal. DeNiro & Hastorf (1985) found little effect of carbonization and early diagenesis on $\delta^{13}C$ over a wide selection of both modern and archaeological plant remains, but they did not tested wood samples. Subsequent studies (Jones & Chaloner, 1991; Czimczik *et al*., 2002) have shown that wood charred at low temperatures (150–300 °C) becomes slightly enriched in $\delta^{13}C$, but exhibits decreasing $\delta^{13}C$ values when carbonized at higher temperatures (300–600 °C). Consequently, $\delta^{13}C$ changes during charcoal formation depend on charring temperature, which in turn determines the degree of carbonization. According to previous studies (e.g. Jones & Chaloner, 1991; Jones *et al*., 1991; Guo & Bustin, 1998; Edwards & Axe, 2004), the usual range of carbonization temperatures appears to be relatively restricted in the fossil record (around 350–450 °C), probably as a compromise between increasing resistance to chemical/biological degradation and decreasing toughness. Nevertheless, and despite the relatively narrow variability in carbonization conditions found within the fossil record, an estimation of the degree of carbonization undergone by archaeological remains seems still necessary in order to consider the use of charcoal $\delta^{13}C$ as a palaeoenvironmental indicator.

Here, we analyzed the effect of carbonization on the $\delta^{13}C$ of Aleppo pine (*Pinus halepensis* Mill.) wood cores collected from nine locations in NE Iberian Peninsula that differed in water availability. *P. halepensis* is a typically drought-avoiding, water-saving species that is highly sensitive to changes in water availability as an adaptive strategy to the large interannual and seasonal variability of Mediterranean climates (Liphschitz & Lev-Yadun, 1986; Ferrio *et al*., 2003a). Besides, previous studies on this species have shown a strong relationship between several indicators of water availability and $\delta^{13}C$ values in wood and its major components, cellulose, and lignin (Ferrio *et al*., 2003a; Ferrio & Voltas, 2005; Klein *et al*., 2005). Our aim was to assess the degree of preservation of these climatic signals in the $\delta^{13}C$ of wood charcoal, and to develop a model to account for the effect (if any) of carbonization. For this purpose, we performed experimental carbonizations over a range of temperatures, and variations in wood $\delta^{13}C$ and carbon concentration (%C) were assessed. The subsequent models were applied to a series of archaeological samples from the Mid Ebro Depression (NE Iberian Peninsula) in order to reconstruct the evolution of aridity in this area during the last 4000 years. This region is among the most arid zones in Europe (annual rainfall between 300 and 400 mm); however, it remains unclear whether present conditions are due to recent environmental changes, or to a progressive aridification which began in prehistoric times. Palaeoenvironmental records for the Late Holocene are still scarce for this area, being mostly derived from pollen and geomorphologic studies (Davis, 1994; Gutiérrez-Elorza & Peña-Monné, 1998; Riera *et al*., 2004). The application of $\delta^{13}C$ analyses to charcoal might provide complementary (and quantitative) data on water availability in the NW Mediterranean Basin. The information obtained is discussed in relation to current knowledge about past climates in the region, and in other areas of Europe and the Mediterranean.

Materials and methods

Reference plant material: tree-ring dating and sample preparation

We sampled wood cores (5.25 mm diameter) of *P. halepensis* Mill. from nine locations in NE Spain that covered a representative range of environmental conditions for this species (Fig. 1, Table 1). Although *P. halepensis* is also found in areas that register up to 800 mm precipitation, we did not include locations with average rainfalls

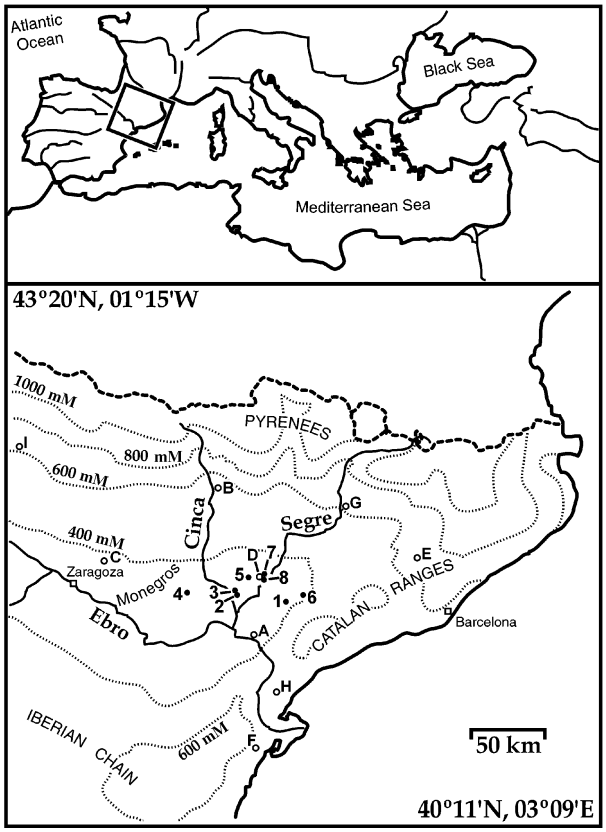

Fig. 1 Geographical distribution of sampling locations for reference wood cores (letters, empty circles), along with archaeological sites where fossil charcoal was collected (numbers, filled circles). For reference, precipitation isohyets are represented. Detailed descriptions of sampling locations and archaeological sites are provided in Tables 1 and 2, respectively.

over 700 mm since above this value, and according to previous studies in the region (Ferrio *et al*., 2003a), wood $\delta^{13}C$ for this species is mostly insensitive to changes in water availability. We selected two healthy, dominant trees per location, and twin cores were taken from the south side of each. Samples were oven-dried at 60 °C for 48 h before being polished to allow tree-ring dating. After visual cross dating, each core was divided in four segments. The number of tree rings included in the segments was variable (2–6) in order to obtain fragments of similar size (10–20 mm length), but all four cores per location followed identical segment division. A total of 154 segments were therefore obtained (nine locations × two trees × two cores × four segments).

Experimental carbonization

For all the analyses, and in order to minimize individual tree effects, we pooled two segments from the same period and location but from distinct trees. Because two cores per tree were taken, for each location we obtained four replicated wood samples, corresponding to four distinct time slices (overall 72 samples). Using direct pairwise comparisons between treatments, these replicates allowed us to assess the effect of a range of carbonization temperatures on $\delta^{13}C$. To this end, we distributed all samples into four subsets of 18 samples each, which were then subjected to distinct carbonization treatments. In particular, one subset was kept as untreated control, whereas the other three were carbonized in a muffle furnace at three maximum temperatures (300 °C, 400 °C, and 500 °C), following the method described by Jones & Chaloner (1991), with slight modifications. The temperatures were chosen to provide material that varied in the degree of carbonization, ranging from slightly charred to fully carbonized (i.e. at the limit of total combustion). In order to emulate the anoxic conditions in which wood becomes charcoal instead of being combusted, samples were heated under restricted oxygen by burying them in metal crucibles under 3 cm of sand. Maximum temperatures were reached after a heating-up time varying from 25 to 35 min (for the 300 °C and the 500 °C treatments, respectively), then the samples were kept in the muffle for 30 min.

Archaeological sites, dating and sample preparation

One hundred and sixty-nine charcoal remains of *P. halepensis* were recovered from seven archaeological sites in the Segre and Cinca Valleys (Mid Ebro Depression, NE Spain, see Fig. 1, Table 2), covering the temporal range between the Bronze Age (ca. 2100 BCE) and Modern Age (XVIII ca. CE). These sites now display similar climate and soil conditions, and are characterized by a semiarid Mediterranean climate. The samples were collected from various archaeological contexts, such as domestic fires, cooking ovens, room floors and levels of rubble from housing structures (for further details about the sites and sampling procedures, see Alonso, 1999, 2005; Alonso *et al*., 2002). Most likely, ancient communities gathered *P. halepensis* close to their settlements, according to the abundance of this species in pollen records (Alonso, 1999) and the poor added value of its wood, which makes worthless any transportation from afar.

For the sites from the Bronze and First Iron period, radiocarbon ages were determined at Beta Analytical Inc. (Miami, FL, USA) and at the Universitat de Barcelona (Barcelona, Spain), and calibrated dating was calculated with the software CALIB REV 4.3 (Stuiver *et al*., 1998). For the remaining sites, a combination of stratigraphic and archaeological dating was used. Radiocarbon dating of individual charcoal fragments

Table 1 Main geographical and environmental variables of sampling locations for reference wood cores

Sampling location	Lat.	Long.	Alt. (m)	P_{an} (mm)	T_{an} (°C)	P/E_{an}
A. Flix	41°15′N	0°32′E	40	389	15.9	0.46
B. El Grado	42°10′N	0°22′E	520	486	13.7	0.64
C. Leciñena	41°48′N	0°28′W	415	368	15.2	0.44
D. Lleida	41°37′N	0°38′E	220	351	14.7	0.44
E. Montserrat	41°34′N	1°47′E	450	387	15.4	0.47
F. Montsià	40°40′N	0°32′E	200	597	17.7	0.66
G. Oliana	42°05′N	1°18′E	480	628	13.9	0.82
H. Rasquera	41°01′N	0°36′E	135	471	15.4	0.59
I. Sos del R.C.	42°28′N	1°15′W	360	609	13.2	0.84

Lat., latitude; Long., longitude; Alt., altitude a.s.l.; Pan, total annual precipitation; Tan, mean annual temperature; P/Ean, ratio between Pan and total annual evapotranspiration (Thornthwaite, 1948).

Table 2 Main geographical and environmental variables (average of present values from the closest meteorological station), dating and cultural period of the archaeological sites

							Calendar year (BCE/CE)		
Archaeological site	Lat.	Long.	Alt. (m)	P_{an} (mm)	T_{an} (°C)	P/E_{an}	Mean	Interval	Cultural period
1. Minferri	41°30′N	0°45′E	240	389	13.5	0.51	1890 cal. BCE	2131–1692 cal. BCE	Bronze Age
							1673 cal. BCE	1879–1517 cal. BCE	
2. Masada de Ratón	41°29′N	0°22′E	130	350	14.6	0.43	1262 cal. BCE	1524–999 cal. BCE	Late Bronze Age
							1110 cal. BCE	1185–982 cal. BCE	
							1062 cal. BCE	1048–936 cal. BCE	
3. Vincamet	41°30′N	0°21′E	110	350	14.6	0.43	988 cal. BCE	1288–928 cal. BCE	Late Bronze Age
4. Tozal de los Regallos	41°30′N	0°01′E	317	359	14.9	0.44	896 cal. BCE	896 cal. BCE	First Iron Age
5. El Vilot de Montagut	41°38′N	0°30′E	250	355	14.7	0.45	888 cal. BCE	1125–795 cal. BCE	Late Bronze Age
							773 cal. BCE	801–396 cal. BCE	
6. Els Vilars	41°34′N	0°56′E	300	403	14.2	0.51	488 BCE	550–425 BCE	Iron (Early Iberian)
7. Roques del Sarró	41°38′N	0°38′E	195	361	14.8	0.46	255 BCE	275–175 BCE	Iron (Iberian)
8. Ciutat de Lleida	41°37′N	0°38′E	220	361	14.8	0.46	26 BCE	50–1 BCE	Roman
							67 CE	20–100 CE	
							200 CE	175–225 CE	
							300 CE	250–350 CE	
							925 CE	900–950 CE	Middle Age
							990 CE	950–1030 CE	
							1010 CE	990–1030 CE	
							1025 CE	950–1100 CE	
							1065 CE	1030–1099 CE	
							1600 CE	1550–1650 CE	Modern Age
							1750 CE	1700–1800 CE	

Lat., latitude; Long., longitude; Alt., altitude a.s.l.; P_{an}, total annual precipitation; T_{an}, mean annual temperature; P/E_{an}, ratio between P_{an} and total annual evapotranspiration (Thornthwaite, 1948); Calendar year, mean values and dating interval (2σ for ^{14}C calibrated -cal. BCE- dates; estimated range for the rest of sites) for each of the sets of samples studied.

was not feasible, so we used average dates for each stratigraphic unit. Nevertheless, *P. halepensis* is a short-living tree (only exceptionally may reach an age over 150 years) and thus age differences between fragments are unlikely to be greater than standard dating intervals. To recover plant remains, soil samples were treated using a standard flotation tank in the field with 5, 2 and 0.5 mm sieves. For the archaeobotanical analyses, charcoal fragments of at least 5 mm were chosen, and taxonomical determinations were performed on the basis of the anatomical features of the wood. For isotope analyses, each charcoal fragment was soaked separately with HCl 6 M for 24 h at room temperature to remove carbonate crusts (DeNiro & Hastorf, 1985). The fragments were then

rinsed repeatedly with distilled water. Carbonate removal is a crucial step not only to avoid shifts in $\delta^{13}C$, but also to achieve a proper determination of charcoal %C.

Carbon concentration and carbon isotope composition

All samples (reference and archaeological) were oven-dried at 60 °C for 24 h and milled to fine powder for carbon isotope analyses. $\delta^{13}C$ and %C were determined by elemental analysis and isotope ratio mass spectrometry (EA/IRMS) at Isotope Services Inc. (Los Alamos, NM, USA). To account for changes in $\delta^{13}C$ of atmospheric CO_2 ($\delta^{13}C_{air}$) during the Holocene, we calculated carbon isotope discrimination in wood ($\Delta^{13}C_w$) from $\delta^{13}C_{air}$ and wood $\delta^{13}C$ ($\delta^{13}C_w$), as described by (Farquhar *et al*., 1982)

$$\Delta^{13}C_w = \frac{\delta^{13}C_{air} - \delta^{13}C_w}{(1 + \delta^{13}C_w/1000)}, \quad (1)$$

$\delta^{13}C_{air}$ was inferred by interpolating a range of data from Antarctic ice-core records (Leuenberger *et al*., 1992; Francey *et al*., 1999; Indermühle *et al*., 1999; Eyer *et al*., 2004; M. Eyer, personal communication), together with modern data from two Antarctic stations (Halley Bay and Palmer Station) of the CU-INSTAAR/NOAA-CMDL network for atmospheric CO_2 measurements (ftp://ftp.cmdl.noaa.gov/ccg/co2c13/flask/readme.html). The whole $\delta^{13}C_{air}$ data set thus obtained covered the period 16 100 BCE—2003 CE. It should be noted that our estimated $\delta^{13}C_{air}$ values (for the Antarctic region) may not exactly correspond with the $\delta^{13}C_{air}$ values for the studied area. However, Antarctic data were the most suitable for our approach, as they provided the most extensive record of long-term global $\delta^{13}C_{air}$ changes. The resulting $\delta^{13}C_{air}$ values applied to extant wood fragments ranged from −8.0‰ to −7.4‰, varying between −6.5‰ and −6.3‰ for fossil charcoal.

Scanning electron microscope (SEM)

As a qualitative assessment of the degree of carbonization in archaeological material, some representative charcoal fragments, along with intact and experimentally carbonized wood, were examined with a SEM. Oven-dried samples were split into 3–4 mm cubic fragments, mounted on SEM stubs, then coated with a gold layer of 26 nm of thickness (ionizer Baltzer SCS 200), and finally examined using a SEM (Zeiss 940) (Carl Zeiss, Oberkochen, Germany).

Meteorological data

Meteorological data were supplied by the Instituto Nacional de Meteorología and the Confederación Hidrográfica del Ebro. We took monthly values for precipitation and temperature within the time period covered by each wood sample used for calibration, and also from 1961 to 1990 for the reference values to characterize present climate at the archaeological sites. From temperature and latitude, potential evapotranspiration was calculated following Thornthwaite (1948). The ratio between precipitation and potential evapotranspiration (P/E) was then calculated as an index of plant water availability.

Statistical analyses

Experimental data were subjected to analysis of variance (ANOVA) to determine the effect of carbonization (fixed factor) and location (random factor) on the $\delta^{13}C$ and %C of wood segments. Linear regressions and covariance analyses were calculated to assess the degree of preservation of the climatic signal in $\delta^{13}C$ after carbonization and the relationship between %C and $\delta^{13}C$ changes, respectively. $\delta^{13}C_{air}$ data from different sources were combined by fitting locally weighted least squares (LOESS) regression curves (span = 0.05, (Cleveland, 1979)), using the proc LOESS included in SAS/STAT v.8 (SAS Institute Inc., Cary, NC, USA). Similarly, we fitted LOESS curves (span = 0.35) to the data sets to objectively summarize overall trends in the time series of estimated climatic variables. Unless otherwise stated, differences were considered statistically significant when $P < 0.05$.

Results

Effect of carbonization on wood appearance, $\delta^{13}C$ and %C

Samples heated at 300 °C ranged in color from very dark brown to matt black, and still retained a strong physical resistance, similar to that from intact wood. When examined with the SEM, we found that cell walls, formed by different layers in control samples (Fig. 2a), became homogeneous at 300 °C (Fig. 2b). With the 400 °C treatment, wood fragments became more brittle (they could be grinded with a mortar) and always showed a bright black color. Under SEM, however, samples looked very similar to those from the 300 °C treatment (Fig. 2c). Finally, the 500 °C treatment originated very brittle, vitreous black fragments of charcoal, so fragile that they disintegrated easily in the course of handling. When examined with SEM, cracking of middle lamella was found widespread, and individual fibers were often pulled apart (Fig. 2d).

For control (untreated) samples, $\delta^{13}C$ showed considerable variation, ranging from −26.14‰ to −22.63‰ (mean = −24.28‰ ± 1.16; herein, mean ± SD), whereas %C showed comparatively less variability (48.2% ± 0.7). The effect of distinct levels of experimental carbonization

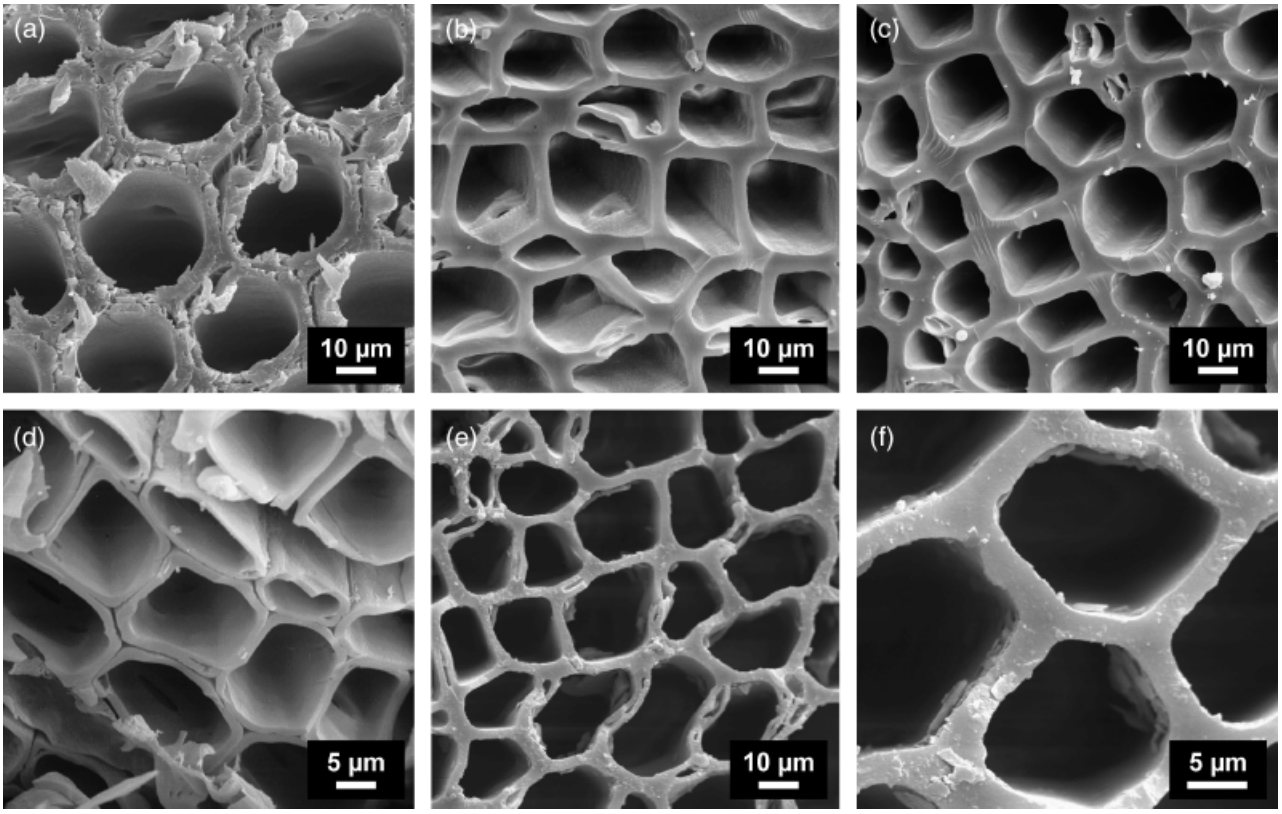

Fig. 2 Scanning electron micrographs of: (a) control samples; (b, c, and d) experimentally carbonized wood at 300 °C, 400 °C, and 500 °C, respectively; (e and f) fossil charcoal fragments from El Vilot de Montagut (773 cal BCE).

(referred to as treatment in Table 3) was significant for $\delta^{13}C$ and %C, although it was far stronger for the latter (the treatment factor explained about 28% and 95% of total variation, respectively, for $\delta^{13}C$ and %C). The geographic origin (location) of samples was still the most determinant factor accounting for $\delta^{13}C$ variation (about 48%), whereas it was not significant for %C. For both variables, the effect of carbonization did not depend on the geographic origin of the samples, as shown by the lack of significant location by treatment interactions. Overall, a significant increase in %C with higher carbonization temperatures was observed, and also a decrease in $\delta^{13}C$ (Fig. 3). Although samples treated at 300 °C showed generally lower $\delta^{13}C$ values ($-24.50\% \pm 1.12$) than controls, they did not differ significantly. Samples treated at 400 °C and 500 °C, however, showed a significantly lower average $\delta^{13}C$ ($-25.67‰ \pm 1.28$ and $-26.15‰ \pm 1.61$, respectively) than controls and samples treated at 300 °C. Furthermore, mean values and within-treatment variability in %C increased from 50.9% ($\pm$ 0.7) at 300 °C to 70.5% ($\pm$ 1.4) and 77.4% ($\pm$ 5.9) at 400 °C and 500 °C, respectively. Because $\delta^{13}C$ and %C showed similar responses to carbonization, we performed a covariance analysis to determine whether variation in %C could explain changes in $\delta^{13}C$ across treatments. After including %C as a covariable in the ANOVA for $\delta^{13}C$, the effect of carbonization was no longer significant ($P = 0.601$), as the covariable explained about 97% of $\delta^{13}C$ variation initially associated with temperature treatments (results not shown).

The relationship between $\delta^{13}C$ in wood before and after charring was studied by pairwise comparisons of replicated samples (i.e. from the same location and time slice) that were simultaneously tested under control and charring conditions. Despite the changes observed in $\delta^{13}C$ after carbonization, the relationship between intact wood and charcoal $\delta^{13}C$ was strongly significant across the three treatments ($r^2 = 0.64$, $P < 0.001$, $N = 18$). Following the results of the covariance analysis, we performed a multiple linear regression (stepwise) to predict original wood $\delta^{13}C$ ($\delta^{13}C_w$) using charcoal $\delta^{13}C$ ($\delta^{13}C_{char}$) and charcoal %C (%C_{char}, surrogate of the impact of carbonization on $\delta^{13}C_w$) as independent variables. Both variables entered the model, giving the following equation:

$$\delta^{13}C_w = -0.706 \times \delta^{13}C_{char} + 0.031 \times \%C_{char} - 8.07,$$
$$r^2 = 0.72,\ P < 0.001,\ N = 18. \quad (2)$$

Table 3 Analysis of variance for the effect of carbonization temperature (treatment) and geographic origin (location) in carbon isotope composition ($\delta^{13}C$) and carbon concentration (%C) of wood

Source	Sum of squares	df	Mean square	*F* ratio	*P* value
$\delta^{13}C$					
Treatment	44.2	3	14.8	22.9	0.000
Location	76.6	8	9.6	14.7	0.000
Treatment × location	15.6	24	0.7	1.0	0.479
Residual	23.2	36	0.6		
%C					
Treatment	11267.7	3	3755.9	492.7	0.000
Location	143.0	8	17.9	2.0	0.095
Treatment × location	217.6	24	9.1	1.2	0.312
Residual	274.4	36	7.6		

The outcome of this model therefore provided estimations of original $\delta^{13}C_w$ from measurements performed on carbonized wood, that is, from $\delta^{13}C_{char}$ and $\%C_{char}$. We applied this equation to fossil material to obtain $\delta^{13}C_w$ estimates directly comparable to intact wood $\delta^{13}C_w$ (see the following sections).

Appearance, $\delta^{13}C$ and %C in archaeological charcoal

Every archaeological specimen was brittle enough to be grinded in a mortar, but in most cases strong enough to be handled without difficulty. After removing carbonate crusts, all the samples were black, although with various degrees of brightness, from nearly matt to a very bright, vitreous appearance. When examined with SEM, cell walls appeared to be homogeneous, with some incipient cracking along the middle lamella (Fig. 2e, f). Raw $\delta^{13}C$ values in charcoal ($\delta^{13}C_{char}$) recovered from archaeological sites ranged from −25.39‰ to −20.85‰, with an average of −23.22‰. Mean values per archaeological site and dating are given in Table 4. The average %C in charcoals was 59.1%, with values varying from 45.0% to 77.1%. After applying Eqn (2), $\delta^{13}C_w$ showed an average value of −22.64‰ (ranging from −24.38‰ to −20.86‰). Carbon isotope discrimination ($\Delta^{13}C_w$), calculated from estimated $\delta^{13}C_w$ and $\delta^{13}C_{air}$, ranged from 14.74‰ to 18.38‰, with an average of 16.55‰. Overall, the archaeological material exhibited higher $\Delta^{13}C_w$ than samples taken from the three locations closer to the area of study and used in the carbonization experiment (average value of 15.79‰; Table 4). For most of the archaeological sites, the variability in $\Delta^{13}C_w$ was similar to that found in experimentally carbonized wood (average within-site standard deviation of 0.71‰ and 0.61‰, for archaeological sites and sampling locations, respectively).

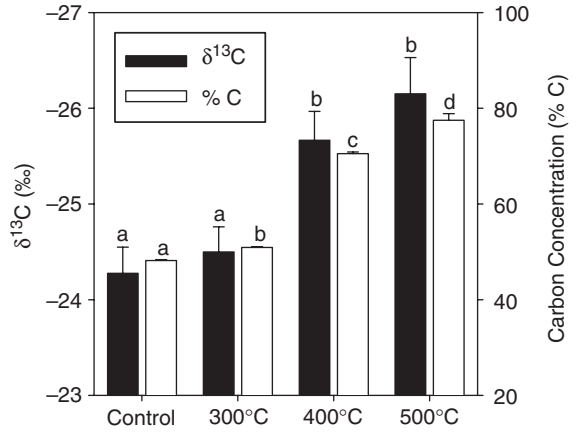

Fig. 3 Mean values and standard error for the $\delta^{13}C$ and %C in intact wood (control) and after carbonization at a range of temperatures. Means with the same letter do not differ significantly on the basis of a least significant difference test ($P < 0.05$).

Estimation of past water availability from the $\Delta^{13}C$ of archaeological charcoal

To assess the implications of $\delta^{13}C$ analysis on charcoals for palaeoclimatic reconstruction, we applied Eqn (2) to the wood segments that had been experimentally carbonized, but for which direct information on intact wood $\delta^{13}C$ values was not available. Estimates of $\delta^{13}C_w$ (from $\delta^{13}C_{char}$ and $\%C_{char}$) were used to calculate $\Delta^{13}C_w$, which were applied to infer climatic variation across the reference locations (nine). No significant relationship between mean annual temperature (T_{an}) and estimated $\Delta^{13}C_w$ was detected. On the contrary, both total annual precipitation (P_{an}) and the ratio between P_{an} and total evapotranspiration (P/E_{an}) were consistently correlated with $\Delta^{13}C_w$ across locations for each temperature treatment ($r = 0.61$–0.96, $P < 0.05$ to $P < 0.001$). Moreover, neither the slope nor the intercept of these relationships differed significantly between treatments, according to a heterogeneity of

Table 4 Average results of the analysis of fossil charcoal for each archaeological site and chronology, compared with experimentally carbonized wood from the three closest sampling locations

Archaeologicalsite/location	Calendar year (BCE/CE)	N	$\delta^{13}C_{air}$ (‰)	$\delta^{13}C_{char}$ (‰)	$\%C_{char}$	Estim. $\delta^{13}C_w$ (‰)	Estim. $\Delta^{13}C_w$ (‰)	Estim. P_{an} (mm)	Estim. P/E_{an}
Fossil charcoal									
1. Minferri	1890 cal. BCE	1	−6.41	−23.73	46.02	−23.40	17.39	576	0.76
1. Minferri	1673 cal. BCE	4	−6.44	−22.58 ± 0.60	47.72 ± 0.81	−22.53 ± 0.40	16.46 ± 0.41	464 ± 50	0.59 ± 0.07
2. Masada de R.	1262 cal. BCE	11	−6.47	−23.28 ± 0.26	50.01 ± 1.09	−22.95 ± 0.18	16.87 ± 0.18	513 ± 22	0.67 ± 0.03
3. Vincamet	1110 cal. BCE	8	−6.47	−23.62 ± 0.14	62.57 ± 2.16	−22.81 ± 0.12	16.72 ± 0.13	495 ± 16	0.64 ± 0.02
2. Masada de R.	1062 cal. BCE	5	−6.48	−23.28 ± 0.30	56.77 ± 3.15	−22.74 ± 0.27	16.64 ± 0.28	486 ± 33	0.63 ± 0.05
2. Masada de R.	988 cal. BCE	8	−6.48	−23.04 ± 0.10	52.93 ± 1.67	−22.70 ± 0.06	16.59 ± 0.06	479 ± 7	0.62 ± 0.01
4. Tozal de los R.	896 cal. BCE	28	−6.48	−23.52 ± 0.17	62.49 ± 1.26	−22.74 ± 0.14	16.63 ± 0.14	484 ± 17	0.62 ± 0.03
5. El Vilot de M.	888 cal. BCE	8	−6.48	−22.79 ± 0.23	58.77 ± 2.82	−22.34 ± 0.21	16.22 ± 0.22	435 ± 26	0.55 ± 0.04
5. El Vilot de M.	773 cal. BCE	9	−6.47	−22.85 ± 0.15	54.97 ± 2.47	−22.49 ± 0.16	16.39 ± 0.17	456 ± 20	0.58 ± 0.03
6. Els Vilars	488 BCE	8	−6.45	−23.23 ± 0.13	57.52 ± 2.89	−22.69 ± 0.12	16.62 ± 0.13	483 ± 15	0.62 ± 0.02
7. Roques del S.	225 BCE	11	−6.42	−22.37 ± 0.40	58.04 ± 2.07	−22.06 ± 0.32	16.00 ± 0.34	409 ± 41	0.51 ± 0.06
8. C. de Lleida	26 BCE	9	−6.39	−23.80 ± 0.21	59.75 ± 2.35	−23.02 ± 0.15	17.03 ± 0.15	532 ± 18	0.69 ± 0.03
8. C. de Lleida	67 CE	6	−6.37	−24.13 ± 0.43	63.62 ± 4.43	−23.13 ± 0.43	17.17 ± 0.45	549 ± 54	0.72 ± 0.08
8. C. de Lleida	200 CE	2	−6.33	−21.80 ± 0.03	59.12 ± 0.10	−21.63 ± 0.02	15.63 ± 0.02	365 ± 2	0.45 ± 0.00
8. C. de Lleida	300 CE	10	−6.33	−23.50 ± 0.12	59.36 ± 1.94	−22.82 ± 0.08	16.88 ± 0.08	515 ± 10	0.67 ± 0.01
8. C. de Lleida	925 CE	9	−6.43	−22.71 ± 0.40	61.22 ± 1.78	−22.20 ± 0.30	16.14 ± 0.31	425 ± 38	0.54 ± 0.06
8. C. de Lleida	990 CE	6	−6.43	−23.66 ± 0.35	60.06 ± 2.47	−22.91 ± 0.29	16.88 ± 0.30	514 ± 36	0.67 ± 0.05
8. C. de Lleida	1010 CE	10	−6.42	−23.42 ± 0.13	61.32 ± 1.96	−22.70 ± 0.12	16.66 ± 0.12	488 ± 15	0.63 ± 0.02
8. C. de Lleida	1025 CE	6	−6.42	−22.44 ± 0.48	62.07 ± 2.14	−21.98 ± 0.33	15.91 ± 0.34	398 ± 41	0.50 ± 0.06
8. C. de Lleida	1065 CE	2	−6.42	−23.03 ± 0.18	57.54 ± 0.14	−22.54 ± 0.12	16.49 ± 0.12	468 ± 15	0.60 ± 0.02
8. C. de Lleida	1600 CE	3	−6.31	−22.99 ± 0.02	64.66 ± 0.88	−22.29 ± 0.04	16.35 ± 0.04	451 ± 5	0.57 ± 0.01
8. C. de Lleida	1750 CE	5	−6.35	−23.80 ± 0.33	66.93 ± 0.31	−22.80 ± 0.23	16.83 ± 0.24	509 ± 29	0.66 ± 0.04
Experimentally carbonized wood									
A. Flix	1985 CE	6	−7.60	−23.60 ± 0.35	63.97 ± 4.45	−22.75 ± 0.24	15.50 ± 0.24	349 ± 29	0.42 ± 0.04
C. Leciñena	1992 CE	6	−7.78	−24.64 ± 0.18	66.32 ± 4.84	−23.41 ± 0.10	16.00 ± 0.12	409 ± 15	0.51 ± 0.02
D. Lleida	1988 CE	6	−7.65	−24.14 ± 0.48	64.57 ± 4.68	−23.11 ± 0.25	15.83 ± 0.26	388 ± 32	0.48 ± 0.05

N, number of samples; $\delta^{13}C_{air}$, average $\delta^{13}C$ in atmospheric CO_2, according to literature data (see text for details); $\delta^{13}C_{char}$, $\delta^{13}C$ values measured in wood charcoals; $\%C_{char}$, carbon concentration, on a dry mass basis; Estim. $\delta^{13}C_w$, estimation of original wood $\delta^{13}C$, following Eqn (2); Estim. $\Delta^{13}C_w$, estimated carbon isotope discrimination of original wood, calculated from $\delta^{13}C_w$ and $\delta^{13}C_{air}$, as described in Eqn (1); Estim. P_{an} and P/E_{an}, average estimates of annual precipitation (P_{an}) and the ratio between P_{an} and evapotranspiration (P/E_{an}) for each site/location, calculated from $\Delta^{13}C_w$ using the models shown in Fig. 4.

slopes ANOVA. Consequently, we averaged $\Delta^{13}C_w$ values across treatments for each location, which are plotted in Fig. 4 together with those reported by Ferrio & Voltas (2005) for intact wood of *P. halepensis* covering a similar ecological gradient (20 locations). The resulting relationships between $\Delta^{13}C_w$ and either P_{an} or P/E_{an} were strongly significant. The slope and intercept terms of the regression lines did not differ significantly from those reported in Ferrio & Voltas, (2005) for intact wood.

Models from Fig. 4 were subsequently applied to estimated $\Delta^{13}C_w$ values of archaeological charcoal in order to infer past trends in water availability (see Table 4). Estimated P_{an} ranged from 257 to 698 mm (478 mm in average), whereas P/E_{an} varied between 0.29 and 0.94, with an average value of 0.61. In both cases, estimated values for archaeological samples were considerably higher than the values recorded for present times, averaged across archaeological sites ($P_{an} = 361$ mm, $P/E_{an} = 0.45$). They were also higher than estimations derived from $\delta^{13}C$ values of present-day wood collected in the same area (Ebro Depression, locations A, C, and D, see Table 4) and experimentally carbonized (estimated $P_{an} = 382$ mm and $P/E_{an} = 0.47$). To avoid possible artifacts in the comparison with present conditions arising from differences in the geographic origin of archaeological samples, we also expressed estimated values as percentage of change with respect to current climatic values at each archaeological site (Table 2, Fig. 5a, b). Mean values of P_{an} and P/E_{an} were predominantly above present-day values, with an average increase of about 33% and 37%, respectively.

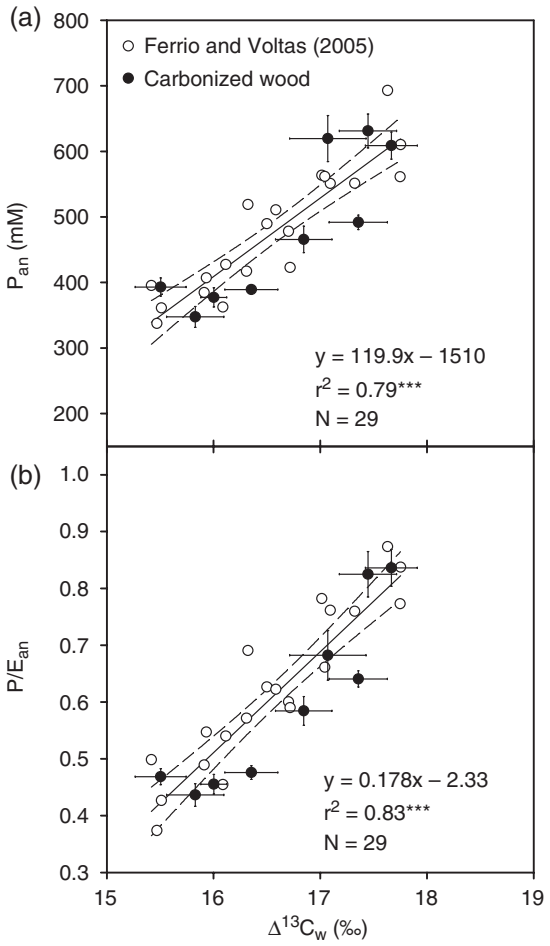

Fig. 4 Relationship between carbon isotope discrimination in wood ($\Delta^{13}C_w$) and either (a) annual precipitation (P_{an}) or (b) the ratio between P_{an} and evapotranspiration (P/E_{an}). Empty circles, intact wood values, as reported by Ferrio & Voltas (2005); filled circles, estimated $\Delta^{13}C_w$ from the analysis of experimentally carbonized wood, as described in Eqn (2). Error bars indicate standard errors for the means.

Discussion

Is the climatic signal of wood $\delta^{13}C$ preserved in charcoal?

The progressively greater depletion in $\delta^{13}C$ with increasing carbonization temperature agrees with the results of earlier studies. For example, Jones and Chaloner (1991) found that wood charred at low temperatures (200 °C) was enriched in $\delta^{13}C$ (+ 0.2‰ in average), whereas at temperatures of 300–500 °C the shift changed to −0.4‰, and at 600 °C it was of −0.8‰. Similar results have been reported by Czimczik *et al*. (2002), who found a slight isotopic enrichment of wood at 150 °C (+ 0.3‰), and a subsequent depletion at 340 °C and 480 °C (from −0.5‰ to −1.1‰). Yet, despite the differences in experimental conditions, there is an overall good concordance among the results from different studies, suggesting that isotopic effects can be linked to the degree of carbonization reached by the samples, regardless of the particular conditions leading to it. Indeed, the response in $\delta^{13}C$ is tightly associated with other physicochemical changes (e.g. reflectance, friability, resistance to oxidation, micromorphology, mass loss, %C) used to describe the degree of carbonization (Jones, 1991; Jones & Chaloner, 1991; Czimczik *et al*., 2002).

Previous studies (Jones, 1991; Czimczik *et al*., 2002) have shown that changes in wood $\delta^{13}C$ after heating can be attributed to the different susceptibility to volatilization of the two major components of wood (cellulose and lignin). Lignin has lower $\delta^{13}C$ than cellulose (e.g. DeNiro & Hastorf, 1985; Borella *et al*., 1998; McCarroll & Loader, 2004; Ferrio & Voltas, 2005), and is less volatile (Kollmann, 1955; Schleser *et al*., 1999; Kaloustian *et al*., 2000). Consequently, charcoal would generally include a greater portion of lignin-derived carbon, causing the observed depletion in $\delta^{13}C$. Nevertheless, because $\delta^{13}C$ displays similar responses to climate in cellulose and

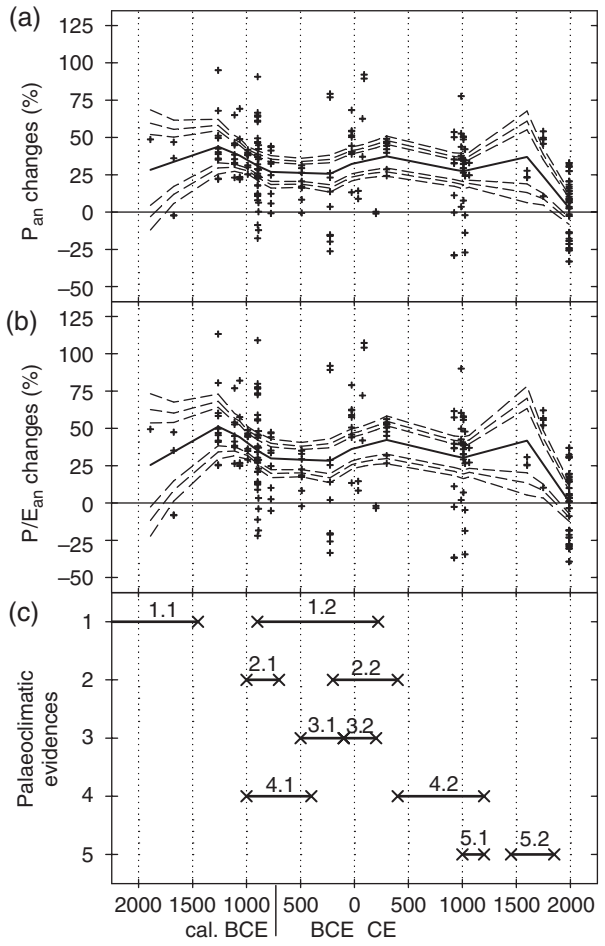

Fig. 5 Estimated evolution of (a) annual precipitation (P_{an}) and (b) the annual mean ratio between P_{an} and evapotranspiration (P/E_{an}), expressed as relative changes (%) respect present climate data. Trend lines depict locally weighted least-squares regression curves (LOESS, span = 0.35) fitted to the data (solid lines), together with their corresponding confidence intervals (99.9%, 99%, and 95%, dashed lines). (c) Chronogram of the main palaeoenvironmental evidences cited in the discussion: 1, Jalut *et al*. (2000); 2, Vernet *et al*. (1996); 3, Magny & Richard (1992); 4, Gutiérrez-Elorza & Peña-Monné (1998); 5, Gribbin & Lamb (1978). Numbered lines indicate the periods mentioned in the text.

lignin (Borella *et al*., 1998; Ferrio & Voltas, 2005), this fractionation during charring would not override the climatic signal of charcoal δ^{13}C. In fact, and despite considerable changes in δ^{13}C during carbonization, our results reveal that the environmental signature of wood δ^{13}C is still present in charcoal. This can be derived not only from the persistence of a geographic signature across a range of heat treatments, but also from the strong correlation between δ^{13}C in intact and carbonized wood. Indeed, we obtained a model to estimate the original δ^{13}C of wood (i.e. before carbonization) from charcoal δ^{13}C, including %C as an indicator of the degree of carbonization. Using this model, we found consistent relationships between Δ^{13}C of carbonized wood (corrected for the effect of carbonization) and climatic variables, and these relationships did not differ significantly from those previously reported for intact wood of *P. halepensis* (Ferrio *et al*., 2003a; Ferrio & Voltas, 2005). Our methodology can be easily implemented in δ^{13}C studies in charcoal, as it does not require further measurements (%C is routinely included in carbon isotope analyses).

The average %C in archaeological samples (59.1%) suggests that most of the samples reached intermediate carbonization levels between the 300 °C and 400 °C treatments. This is further confirmed by the similarities in appearance and anatomical features between most archaeological specimens and the samples derived from these treatments (see Fig. 2). This observation is consistent with evidence from previous anatomical studies and spectral measurements (Jones & Chaloner, 1991; Jones *et al*., 1991; Guo & Bustin, 1998; Edwards & Axe, 2004), thereby indicating that most of the fossil charcoal was formed between ca. 350 °C and 450 °C. Given that this 'optimal' temperature range for charcoal preservation was well covered by our experiment, the resulting model to estimate original δ^{13}C from charcoal would be, in principle, applicable to most archaeological samples. Nevertheless, as δ^{13}C changes observed during carbonization are mostly attributable to differential combustion of lignin and cellulose, and their amounts and chemical attributes may differ among species (e.g. Kollmann, 1955; Czimczik *et al*., 2002), this particular model might not be directly applicable to other species, mainly nonconifers.

Potential sources of error in estimating past water availability from Δ^{13}C

Although precipitation/evapotranspiration regimes are by far the most important factors determining Δ^{13}C in *P. halepensis* (Ferrio *et al*., 2003a; Ferrio & Voltas, 2005; Klein *et al*., 2005), we cannot obviate the potential effect of other variables on Δ^{13}C. Firstly, temperature changes might affect the growing cycle, thus affecting effective tree water availability, regardless of the overall annual precipitation. For example, low winter temperatures reduce the growing cycle of *P. halepensis*, as it is sensitive to cold and can virtually arrest growth during the cold season (Liphschitz & Lev-Yadun, 1986). This kind of responses may cause a reduction in effective water uptake by trees, not necessarily reflected in precipitation records, and thus should be considered when interpreting isotope results. On the other hand, several site parameters, such as altitude, slope and aspect, soil

type, or canopy density, may also affect $\Delta^{13}C$ (see references in McCarroll & Loader, 2004; Ferrio *et al*., 2005b). However, such differences are relatively small as compared with climatic effects (generally below 0.5‰), especially within a rather uniform area, as is our case. Finally, we should consider the inherent risk of using present $\Delta^{13}C$–climate relationships to reconstruct water availability from the archaeological record, as recent increases in CO_2 partial pressure might have a direct effect on $\Delta^{13}C$ values. In this sense, experimental studies under controlled environments have shown that $\Delta^{13}C$ of a variety of C_3 plants suffers little change over a wide range of CO_2 partial pressures (Polley *et al*., 1993; Beerling & Woodward, 1995; Picon *et al*., 1996). In most cases, the increase in assimilation rates was compensated by a decrease in stomatal conductance, thus minimizing variations in the ratio of intercellular to atmospheric partial pressure of CO_2, and, thus, in $\Delta^{13}C$. Moreover, the relationship between stomatal conductance and plant water status is comparable under different CO_2 concentrations (e.g. Picon *et al*., 1996; Bunce, 2004). Overall, these results indicate that $\Delta^{13}C$ can be useful to estimate past water availability, regardless of atmospheric CO_2 changes.

Changes in aridity during the last 4000 years in the NW Mediterranean Basin

In spite of the aforementioned factors, our approach provided a robust quantification of climatic variables directly associated with water availability, such as P_{an} and P/E_{an}. This methodology makes the comparison between past and present-day conditions easier than the most common qualitative or semiquantitative approaches (see references in IPCC, 2001). In our study, estimated P_{an} and P/E_{an} from the analysis of charcoal $\delta^{13}C$ were significantly higher in the past than in present times, and showed an increase over 30% in relation to current values. These results were supported by $\delta^{13}C$ analysis of experimentally carbonized wood from three reference locations (A, C, and D in Tables 1 and 4), as these sites provided significantly lower estimations of P_{an} and P/E_{an} than the average for archaeological samples. Moreover, the good agreement between recorded and $\delta^{13}C$-based values across the three reference locations further supports the validity of our models (estimated $P_{an} = 382\,mm$ and $P/E_{an} = 0.47$, climatic data $P_{an} = 379\,mm$ and $P/E_{an} = 0.48$).

On the basis of these findings, present-day semiarid conditions in the region may be mostly due to recent climatic shifts towards a harsher climate, probably enhanced by anthropogenic disturbance. A considerable decrease in precipitation in NW Mediterranean has been reported after 1850, as shown by tree-ring analyses (Creus *et al*., 1996), lake-level records (Riera *et al*., 2004), and documentary studies (Barriendos & Martín-Vide, 1998). In addition to a fall in precipitation, the global increase in temperature since the mid-XIXth century has augmented plant water demand, and, consequently, water stress, throughout the Mediterranean Region (Creus *et al*., 1996; IPCC, 2001).

In addition to the overall differences between past and present-day values, two main phases of greater water availability alternating with drier periods were detected (see Fig. 5a, b). The first humid phase (1500–900 BCE) gave significantly higher averages of P_{an} and P/E_{an} than those for the present (increase of 39% and 46%, respectively). This humid period coincided with the interphase between two aridification periods (2350–1450 BCE and 900 BCE–220 CE, 1.1 and 1.2 in Fig. 5c) as defined by Jalut *et al*. (2000) for NW Mediterranean on the basis of a transect of pollen analyses. Because of the small number of samples available, the relatively arid episode described by Jalut *et al*. (2000) around 2350–1450 BCE was not well characterized in our data. Nevertheless, we found a trend towards lower water availability from 2000 to 1500 BCE (when compared with the following period) although, on average, P_{an} and P/E_{an} estimated for this period were still higher than present-day values.

The most consistent arid phase within the timeframe of this study corresponded to the period 900–300 BCE (Fig. 5a, b). Nevertheless, even in this phase, our estimates of water availability were significantly higher than for present times (about 24%). This period was followed by a recovery of water availability between 300 BCE and 300 CE, with average P_{an} and P/E_{an} about 35% and 39% higher than present-day values. The analysis of $\delta^{13}C$ in charcoals from a Mediterranean deciduous oak (*Quercus pubescens* W.) performed by Vernet *et al*. (1996) in Southern France also indicated a period of lower water availability ca. 3000–2700 BP (2.1 in Fig 5C), a subsequent recovery ca. 2200–1600 BP (2.2 in Fig 5c), and a declining trend onwards until present times. Furthermore, pollen analyses performed at the archaeological site of El Vilot de Montagut (Alonso *et al*., 2002) revealed an increase in aridity at the beginning of the third millennium, which is in agreement with the low $\Delta^{13}C$ values found for this site. Likewise, the humid phase between 300 BCE and 300 CE was also confirmed by pollen data from the city of Lleida (0–200 CE), which indicated a relatively wet climate (S. Riera, unpublished results). Similarly, lower groundwater fluxes from 500 to 100 BCE than between 100 BCE and 200 CE have been reported (Magny & Richard, 1992; 3.1 and 3.2 in Fig. 5c). Some studies, however, provide apparently contradictory results for the arid period 900–300 BCE. Geomorphologic studies throughout the

Ebro Basin (Gutiérrez-Elorza & Peña-Monné, 1998) report a generalized decrease in soil erosion around 1000–400 BCE (4.1 in Fig. 5c), which was interpreted as an increase in vegetation cover, and a colder/wetter climate. This is partly supported by vegetation reconstructions (based on charcoal analyses) from the Cinca and Segre Valleys (Alonso, 1999) reporting evidences of mixed forests of holm oaks, pines and deciduous oaks (i.e. colder/wetter climate than today). The most probable explanation for such divergent results might be found in the aforementioned reduction of the growing cycle of *P. halepensis* in response to low temperatures, increasing its reliance on summer rainfall. Moreover, lower temperatures might also have reduced the incidence of convective storms (therefore decreasing water availability) from late spring to early autumn (Gribbin & Lamb, 1978). Indeed, $\Delta^{13}C$ analyses of cereal grains (Araus & Buxó, 1993; Araus *et al*., 1997; Ferrio *et al*., 2005a) indicate that water inputs during grain filling (late spring) decreased significantly during this period in NW Mediterranean. Thus, a combination of colder/wetter winters with drier summers might be the cause for the observed increase in water stress for *P. halepensis* during this period. This hypothesis is further confirmed by the archaeobotanical record from the nearby Monegros region, showing an increase in continentality, evidenced by the disappearance of cold-sensitive species (Alonso, 1999). Under such scenario, our findings would be fully compatible with a reduction of soil erosion (Gutiérrez-Elorza & Peña-Monné, 1998), enhanced by the absence of convective storms, without discarding an increase in vegetation cover, driven by cold-resistant species with deep-root systems to exploit winter-fed water reservoirs (e.g. Mediterranean oaks; Alonso, 1999). Expanding $\Delta^{13}C$ analyses to these species might help to elucidate the origin of these contrasting results, and provide useful information on the seasonality of precipitation events.

After a gap in the archaeological record between 300 and 900 CE, we identified a third period (900–1100 CE) with a strong variability and relatively dry climate, but still wetter than today (Fig. 5a, b). This coincides with the Medieval Warm Period (Gribbin & Lamb, 1978; 1000–1200 CE; 5.1 in Fig. 5c), characterized by an overall increase in temperature and climate unstability. Pollen data from the city of Lleida also indicate drier conditions in this period than at the beginning of the first Millennium CE (S. Riera, unpublished results), and documentary studies reflect a climate with strong interannual contrasts, alternating drought periods with catastrophic floods (Gargallo, 1989). Furthermore, soil erosion increased around 400–1200 CE (Gutiérrez-Elorza & Peña-Monné, 1998; 4.2 in Fig. 5c), which is consistent with a more arid and variable climate. Our analyses revealed a subsequent recovery in water availability from the XVIth to the XVIIIth century (35–39% over current values, see Fig. 5a, b), although, because of the small number of samples available, these results are not conclusive. Nevertheless, this period coincides with the Little Ice Age (Gribbin & Lamb, 1978; 1450–1850 CE; 5.2 in Fig. 5c), characterized by lower mean temperatures, a strong climatic variability and increased lake levels (Creus *et al*., 1996; Barriendos & Martín-Vide, 1998; Riera *et al*., 2004), together with reduced soil erosion (Gutiérrez-Elorza & Peña-Monné, 1998).

Conclusions

Our experimental data demonstrate that the climatic signal of wood $\delta^{13}C$ is preserved after carbonization, and that shifts in $\delta^{13}C$ caused by this process can be successfully removed. Moreover, the generally good agreement between our findings and evidence provided by several palaeoenvironmental data from NW Mediterranean supports the usefulness of $\delta^{13}C$ analysis in wood charcoal to expand current palaeoclimatic records, especially in dry areas where other records (e.g. lake sediments, ice cores, tree rings) are relatively scarce. Even in regions where long palaeoclimatic records are available, $\delta^{13}C$ in charcoal might provide a complementary (and quantitative) source of information, in order to achieve a greater understanding of past climate dynamics. The divergences between our results and some palaeoenvironmental evidences, however, highlight the complexity of combining information from distinct sources. Nevertheless, interdisciplinarity is an essential prerequisite for palaeoenvironmental studies, as each proxy has its own constraints, which can be overcome only by considering alternative inferential sources. In this regard, the physiological characteristics of the species examined must be considered to ensure a proper interpretation of $\delta^{13}C$ trends in fossil charcoal.

Acknowledgements

This study was supported by the projects DGI CGL2005–08175-C02–02/BOS and MENMED (INCO-MED-ICA3-CT-2002–10022). We thank M. Ros and R. Piqué for performing charcoal determinations, A. Florit, A. Vega and J. Coello for assistance in sampling preparation, and F. Rodriguez for useful suggestions regarding statistics. We also thank the excavation teams from Masada de Ratón (J. Rey), Tozal de los Regallos (S. Melguizo), the *Servei Municipal d'Arqueologia de Lleida*, and the staff from the *Grup d'Investigació Prehistòrica* for their work and financial support for sampling dating. We also thank the comments from D. Gröcke and one anonymous referee, which helped us to improve substantially the initial manuscript. J. P. Ferrio had a PhD fellowship from the Generalitat de Catalunya.

References

Alonso N (1999) De la llavor a la farina: els processos agrícoles protohistòrics a la catalunya occidental. UMR 154-CNRS, Lattes.

Alonso N (2005) Roman and islamic plant remains from the city of lleida (Catalonia, Spain). *Vegetation History and Archaeobotany*, **14**, 341–361.

Alonso N, Gené M, Junyent E *et al*. (2002) Recuperant el passat a la línia del Tren d'Alta Velocitat. L'assentament protohistòric, medieval i d'època moderna de El Vilot de Montagut (Alcarràs, Lleida). GIF, Generalitat de Catalunya, Lleida.

Araus JL, Buxó R (1993) Changes in carbon isotope discrimination in grain cereals from the north-western mediterranean basin during the past seven millennia. *Australian Journal of Plant Physiology*, **20**, 117–128.

Araus JL, Febrero A, Buxó R *et al*. (1997) Changes in carbon isotope discrimination in grain cereals from different regions of the western Mediterranean basin during the past seven millennia. Palaeoenvironmental evidence of a differential change in aridity during the late holocene. *Global Change Biology*, **3**, 107–118.

Barriendos M, Martín-Vide J (1998) Secular climatic oscillations as indicated by catastrophic floods in the Spanish mediterranean coastal area (14th–19th centuries). *Climatic Change*, **38**, 473–491.

Beerling DJ, Woodward FI (1995) Leaf stable carbon isotope composition records increased water-use efficiency of C_3 plants in response to atmospheric CO_2 enrichment. *Functional Ecology*, **9**, 394–401.

Borella S, Leuenberger M, Saurer M *et al*. (1998) Reducing uncertainties in $\delta^{13}C$ analysis of tree rings: pooling, milling, and cellulose extraction. *Journal of Geophysical Research*, **103**, 19,519–19,526.

Bunce JA (2004) Carbon dioxide effects on stomatal responses to the environment and water use by crops under field conditions. *Oecologia*, **140**, 1–10.

Cleveland WS (1979) Robust locally weighted regression and smoothing scatterplots. *Journal of the American Statistical Association*, **74**, 829–836.

Creus J, Fernández-Cancio A, Manrique-Menéndez E (1996) Evoluciòn de la temperatura y precipitación anuales desde el año 1400 en el sector central de la Depresión del Ebro. *Lucas Mallada*, **8**, 9–27.

Czimczik CI, Preston CM, Schmidt MWI *et al*. (2002) Effects of charring on mass, organic carbon, and stable carbon isotope composition of wood. *Organic Geochemistry*, **33**, 1207–1223.

Davis BAS (1994) *Palaeolimnology and Holocene environmental change from endorreic lakes in the Ebro Basin, N.E. Spain*. PhD thesis, University of Newcastle upon Tyne.

DeNiro MJ, Hastorf CA (1985) Alteration of $^{15}N/^{14}N$ and $^{13}C/^{12}C$ ratios of plant matter during the initial stages of diagenesis: studies utilizing archaeological specimens from peru. *Geochimica et Cosmochimica Acta*, **49**, 97–115.

Edwards D, Axe L (2004) Anatomical evidence in the detection of the earliest wildfires. *Palaios*, **19**, 113–128.

Eyer M, Leuenberger M, Nyfeler P *et al*. (2004) Comparison of two $\delta^{13}CO_2$ records measured on air from the EPICA Dome C and Kohnen station cores. *Geophysical Research Abstracts*, **6**, 1990.

Farquhar GD, O'Leary MH, Berry JA (1982) On the relationship between carbon isotope discrimination and the intercellular carbon dioxide concentration in leaves. *Australian Journal of Plant Physiology*, **9**, 121–137.

February EC, Van der Merwe NJ (1992) Stable carbon isotope ratios of wood charcoal during the past 4000 years: anthropogenic and climatic influences. *South African Journal of Science*, **88**, 291–292.

Ferrio JP, Araus JL, Buxó R *et al*. (2005a) Water management practices and climate in ancient agriculture: inference from the stable isotope composition of archaeobotanical remains. *Vegetation History and Archaeobotany*, **14**, 510–517.

Ferrio JP, Florit A, Vega A *et al*. (2003a) $\Delta^{13}C$ and tree-ring width reflect different drought responses in *Quercus ilex* and *Pinus halepensis*. *Oecologia*, **137**, 512–518.

Ferrio JP, Resco V, Williams DG *et al*. (2005b) Stable isotopes in arid and semi-arid forest systems. *Investigación Agraria, Sistemas y Recursos Forestales*, **14**, 371–382.

Ferrio JP, Voltas J (2005) Carbon and oxygen isotope ratios in wood constituents of *Pinus halepensis* as indicators of precipitation, temperature and vapour pressure deficit. *Tellus Series B – Chemical and Physical Meteorology*, **57B**, 164–173.

Ferrio JP, Voltas J, Araus JL (2003b) Use of carbon isotope composition in monitoring environmental changes. *Management of Environmental Quality*, **14**, 82–98.

Figueiral I, Terral JF (2002) Late quaternary refugia of Mediterranean taxa in the portuguese estremadura: charcoal based palaeovegetation and climatic reconstruction. *Quaternary Science Reviews*, **21**, 549–558.

Francey RJ, Allison CE, Etheridge DM *et al*. (1999) A 1000-year high precision record of delta C-13 in atmospheric CO_2. *Tellus Series B – Chemical and Physical Meteorology*, **51**, 170–193.

Gargallo A (1989) *El concejo de Teruel en la Edad Media (1177–1327)*. PhD thesis, University of Zaragoza.

Gribbin J, Lamb HH (1978) Climatic change in historical times. In: *Climatic Change* (ed. Gribbin J), pp. 68–82. Cambridge University Press, Cambridge.

Gröcke DR (1998) Carbon-isotope analyses of fossil plants as a chemostratigraphic and palaeoenviromental tool. *Lethaia*, **31**, 1–13.

Gröcke DR (2002) The carbon isotope composition of ancient CO_2 based on higher-plant organic matter. *Philosophical Transactions of the Royal Society of London*, **A360**, 633–658.

Guo Y, Bustin RM (1998) FTIR spectroscopy and reflectance of modern charcoals and fungal decayed woods: implications for studies of inertinite in coals. *International Journal of Coal Geology*, **37**, 29–53.

Gutiérrez-Elorza M, Peña-Monné JL (1998) Geomorphology and late Holocene climatic change in northeastern Spain. *Geomorphology*, **23**, 205–217.

Indermühle A, Stocker TF, Joos F *et al*. (1999) Holocene carbon-cycle dynamics based on CO_2 trapped in ice at Taylor dome, Antarctica. *Nature*, **398**, 121–126.

IPCC (2001) *Climate Change 2001: the Scientific Basis*. Cambridge University Press, Cambridge.

Jalut G, Esteban-Amat A, Bonnet L *et al*. (2000) Holocene climatic changes in the western mediterranean, from south-east France to south-east Spain. *Palaeogeography Palaeoclimatology Palaeoecology*, **160**, 255–290.

Jones TP (1991) *The nature, origin and recognition of fusain*. PhD thesis, Univ London.

Jones TP, Chaloner WG (1991) Fossil charcoal, its recognition and palaeoatmospheric significance. *Palaeogeography, Palaeoclimatology, Palaeoecology*, **97**, 39–50.

Jones TP, Scott AC, Cope M (1991) Reflectance measurements and the temperature of formation of modern charcoals and implications for studies of fusain. *Bulletin de la Societe Géologique de France*, **162**, 193–200.

Kaloustian J, Pauli AM, Pastor J (2000) Decomposition of biopolymers of some mediterranean plants during heating. *Journal of Thermal Analysis and Calorimetry*, **61**, 13–21.

Klein T, Hemming D, Lin T *et al*. (2005) Association between tree-ring and needle $\delta^{13}C$ and leaf gas exchange in *Pinus halepensis* under semi-arid conditions. *Oecologia*, **144**, 45–54.

Kollmann F (1955) *Technologie Des Holzes Und Der Holzwerkstoffe*. Springer Verlag, Heidelberg.

Leuenberger M, Siegenthaler U, Langway CC (1992) Carbon isotope composition of atmospheric CO_2 during the last ice age from an antartic ice core. *Nature*, **357**, 488–490.

Liphschitz N, Lev-Yadun S (1986) Cambial activity of evergreen and seasonal dimorphics around the mediterranean. *IAWA Bulletin*, **7**, 145–153.

Magny M, Begeot C, Guiot J *et al*. (2003) Contrasting patterns of hydrological changes in Europe in response to Holocene climate cooling phases. *Quaternary Science Reviews*, **22**, 1589–1596.

Magny M, Richard H (1992) Essai de synthèse vers une courbe de l'évolution du climat entre 500BC et 500AD. *Les nouvelles de l'archéologie*, **50**, 58–60.

McCarroll D, Loader NJ (2004) Stable isotopes in tree rings. *Quaternary Science Reviews*, **23**, 771–801.

Picon C, Guehl JM, Ferhi A (1996) Leaf gas exchange and carbon isotope composition responses to drought in a drought-avoiding (*Pinus pinaster*) and a drought-tolerant (*Quercus petraea*) species under present and elevated atmospheric CO_2 concentrations. *Plant, Cell and Environment*, **19**, 182–190.

Polley HW, Johnson HB, Marino BD *et al*. (1993) Increase in C_3 plant water-use efficiency and biomass over Glacial to present CO_2 concentrations. *Nature*, **361**, 61–64.

Riera S, Wansard G, Julià R (2004) 2000-year environmental history of a karstic lake in the Mediterranean Pre-Pyrenees: the Estanya lakes (Spain). *Catena*, **55**, 293–324.

Rodó X, Baert E, Comin FA (1997) Variations in seasonal rainfall in southern Europe during the present century: relationships with the north atlantic oscillation and the el niño southern oscillation. *Climate Dynamics*, **13**, 275–284.

Schleser GH, Frielingsdorf J, Blair A (1999) Carbon isotope behaviour in wood and cellulose during artificial aging. *Chemical Geology*, **158**, 121–130.

Stuiver M, Reimer PJ, Bard E *et al*. (1998) INTCAL98 radiocarbon age calibration, 24,000–0 cal BP. *Radiocarbon*, **40**, 1041–1083.

Thornthwaite CW (1948) An approach towards a rational classification of climate. *Geographical Review*, **38**, 55–94.

Van Bergen PF, Poole I (2002) Stable carbon isotopes of wood: a clue to palaeoclimate? *Palaeogeography Palaeoclimatology Palaeoecology*, **182**, 31–45.

Vernet JL, Pachiaudi C, Bazile F *et al*. (1996) Le $\delta^{13}C$ de charbons de bois préhistoriques et historiques méditerranéens, de 35000 BP a l'àctuel. Premiers resultats. *Comptes Rendus de l'Academie des Sciences, série II a*, **323**, 319–324.

Willcox G (1999) Charcoal analysis and Holocene vegetation history in southern Syria. *Quaternary Science Reviews*, **18**, 711–716.